Shell structure in large nonspherical metal clusters

J. Mansikka-aho, E. Hammarén, and M. Manninen
Department of Physics, University of Jyväskylä, P.O. Box 35, SF-40351 Jyväskylä, Finland
(Received 26 December 1991)

Electronic shell structure of icosahedral and cuboctahedral sodium clusters with 300 to 1500 atoms has been studied using a potential-well approximation for the effective one-electron potential. The results show that icosahedral clusters yield the same shell structure as spherical clusters up to the cluster size of about 500 atoms and that similarities persist until the cluster has about 1000 atoms. The shell structure of a cuboctahedral geometry begins to deviate from that of a sphere when the cluster size is about 100. A study on quadrupole deformations of large clusters shows that surface fluctuations in liquid clusters cannot destroy the shell structure even in the largest clusters.

I. INTRODUCTION

The simplest model for the electronic structure of the alkali-metal clusters is the jellium model.[1-5] It accounts for the major magic numbers seen most clearly in the mass spectra.[6,7] The magic numbers result from the shell structure of the valence electrons: a shell closing corresponds to a magic cluster. In the spherical jellium model, the local-density approximation of the Kohn-Sham density-functional formalism[8,4] is usually used for determining the single-electron levels. The electrons then move in a spherical effective potential that, for large clusters, resembles a square well with a rounded edge.[3] This potential dictates basic features of the observed shell structure, whereas details depend on the exact shape of the self-consistent potential.[9]

Recently, an additional set of magic numbers for large simple metal clusters has been observed.[10-12] These correspond to the geometrical packing of atoms in an icosahedral structure: complete icosahedral give the major magic numbers. It is interesting to note that in the case of sodium clusters the magic numbers in the same size region (1500–3000 atoms) can be determined either by the electronic structure[7] or by the geometry,[10] depending upon the experimental conditions.

The purpose of the present paper is to study the effect of the cluster geometry on the electronic-shell structure. Two questions are addressed: (i) what is the shell structure in icosahedral and cuboctahedral metal clusters and (ii) how do the surface fluctuations affect the shell structure in liquid clusters? This work is a continuation of an earlier work[13] where a simple Hückel model was applied to study the effect of the surface faceting on the shell structure. The results indicated that the icosahedral symmetry can keep up the shell structure even if the cluster has hundreds of atoms. Our present results show that in the first supershell[9,5] the main features of the spherical shell structure are seen also in the icosahedral clusters. However, in the second supershell the icosahedral clusters will have very different shell closings.

It should be stressed that we are solely concentrating on the existence of the electronic-shell structure in the clusters and we do not try to calculate the total energy for different geometries. The latter is needed in determining the most stable cluster sizes and geometries. For the smallest clusters, *ab initio* methods have been used for calculating the total energies[14,15] and approximative methods have been applied for larger clusters.[16-18]

For liquid clusters the surface tension forces the large clusters to be spherical. However, due to the finite temperature the surface of the cluster can oscillate. We have estimated the effect of these surface fluctuations on the electronic-shell structure. With simple arguments and model calculations, we show that the surface oscillations of liquid sodium clusters do not have any marked effect on the shell structure, and that the relative effect of the surface oscillations to the shell structure becomes smaller when the cluster size increases.

The plan of the paper is as follows. In Sec. II we will describe the theoretical model. The shell structure of icosahedral and cuboctahedral clusters is discussed in Sec. III. Section IV studies quadrupole deformations and their relation to the liquid clusters. Section V gives the conclusions.

II. ELECTRONIC LEVELS IN A NONSPHERICAL POTENTIAL WELL

For large sodium clusters, the effective potential of the electrons inside the cluster is nearly constant and the effect of the ionic pseudopotentials on the shell structure is vanishingly small.[19] In order to study the effect of the geometry of the effective potential, we mimic the clusters with finite potential wells having required shapes. The depth of a well is determined by

$$V_0 = -\phi - \epsilon_F \ , \tag{1}$$

where ϕ is the work function of the metal and ϵ_F the Fermi energy of a bulk free-electron metal measured from the bottom of the conduction band. For spherical clusters, the radius is determined by $r_0 = N^{1/3} r_s$, where N is the number of atoms in the cluster and r_s the Wigner-Seitz radius. All calculations in this paper have been done with the parameters for sodium: $V_0 = -0.205$ a.u. and $r_s = 3.93$ a.u.

The nonspherical clusters are described by using nonspherical potential wells with the same depth, Eq. (1), and volume as the spherical cluster having an equal number of atoms. The difference between the spherical and nonspherical potentials is restricted within a narrow region close to the cluster surface. It is then natural to solve the Schrödinger equation for the nonspherical case by using as a basis set the solutions for the spherical potential well:

$$\psi_{nlm}(\mathbf{r})=R_{nl}(r)Y_{lm}(\theta,\phi) , \tag{2}$$

where $Y_{lm}(\theta,\phi)$ are the spherical harmonics. The radial wave function (spherical Bessel function inside the cluster) and the corresponding energy eigenvalue are obtained numerically.

The difference between the potentials of spherical and nonspherical clusters is defined as

$$\Delta V(\bar{r})=V_0\{\theta[R(\theta,\phi)-r]-\theta(r_0-r)\} , \tag{3}$$

where θ is the step function. The angle-dependent distance $R(\theta,\phi)$ is defined as the distance from the center of the cluster to its surface. The energy eigenvalues for the nonspherical potential well can now be obtained by diagonalizing the Hamiltonian matrix

$$\langle nlm|H_0+\Delta V|n'l'm'\rangle , \tag{4}$$

where H_0 is the single-particle Hamiltonian for the spherical potential well.

Because the perturbation potential of Eq. (3) is nonzero only close to the radius r_0, it is convenient to expand the radial wave function as

$$R_{nl}(r)=R_{nl}(r_0)+R'_{nl}(r_0)(r-r_0) , \tag{5}$$

where R'_{nl} is the derivative of R_{nl}. The matrix elements of the perturbation now give two terms

$$\langle nlm|\Delta V|n'l'm'\rangle=\langle V\rangle_0+\langle V\rangle_1 , \tag{6}$$

where

$$\langle V\rangle_0=V_0r_0^3R_{nl}(r_0)R_{n'l'}(r_0)M^0_{ll'(m-m')} \tag{7}$$

and

$$\langle V\rangle_1=V_0r_0^4[R_{nl}(r_0)R'_{n'l'}(r_0)+R'_{nl}(r_0)R_{n'l'}(r_0)]M^1_{ll'(m-m')} . \tag{8}$$

Here the matrix elements $M^\nu_{ll'(m-m')}$ over the angle variables are defined as

$$M^\nu_{ll'(m-m')}=\int d\theta\sin\theta Q_{lm}(\theta)Q_{l'm'}(\theta)\times\int d\phi\cos[(m-m')\phi]I_\nu(\theta,\phi) , \tag{9}$$

where $Q_{lm}(\theta)=Y_{lm}(\theta,\phi)/e^{im\phi}$ and the functions $I_\nu(\theta,\phi)$ are

$$I_0(\theta,\phi)=\frac{1}{3r_0^3}[R(\theta,\phi)^3-r_0^3] \tag{10}$$

and

$$I_1(\theta,\phi)=\frac{1}{12}+\frac{1}{4}\frac{R(\theta,\phi)^4}{r_0^4}-\frac{1}{3}\frac{R(\theta,\phi)^3}{r_0^3} . \tag{11}$$

Group theory dictates the maximum degeneracy a state can have in a given symmetry. For the cuboctahedral symmetry the maximum degeneracy is three and for the icosahedral symmetry it is five. If the potential well has an icosahedral symmetry, it has a five axis and the matrix elements of M^ν are nonzero only if $|m-m'|$ is 0,5,10, etc. For cuboctahedral symmetry, due to the four axis, M^ν is nonzero only if $|m-m'|$ is 0,4,8, etc.

The advantage of the approximation (3) is that the M matrix depends only on the angle variables of the wave function and thus on the geometry of the cluster (but not its size). The disadvantage is that only relatively small deformations of the sphere can be calculated accurately. By comparing the Fermi wavelength to the maximum change in the cluster radius $R(\theta,\phi)$ we have estimated that the results for icosahedral with more than about 1500 atoms and cuboctahedra with more than about 1000 atoms could already be affected by this approximation.

The energy levels for the 309-atom cluster have been calculated by including in the Hamiltonian matrix all the bound states in the spherical potential well. For larger clusters only a limited number of basis functions close to the Fermi level was used. For the 561-, 923-, and 1415-atom icosahedral clusters we used 33, 29, and 23 nl states around the Fermi level, respectively. Consequently in each case the total number of nlm-basis functions was about 450.

III. SHELL STRUCTURE IN ICOSAHEDRAL AND CUBOCTAHEDRAL CLUSTERS

Using the above-described model of a finite potential well, we have calculated the electronic structure of complete icosahedral and cuboctahedral sodium clusters with 309, 561, 923, and 1415 atoms. Figure 1 shows the electronic-shell structures for spherical, icosahedral, and

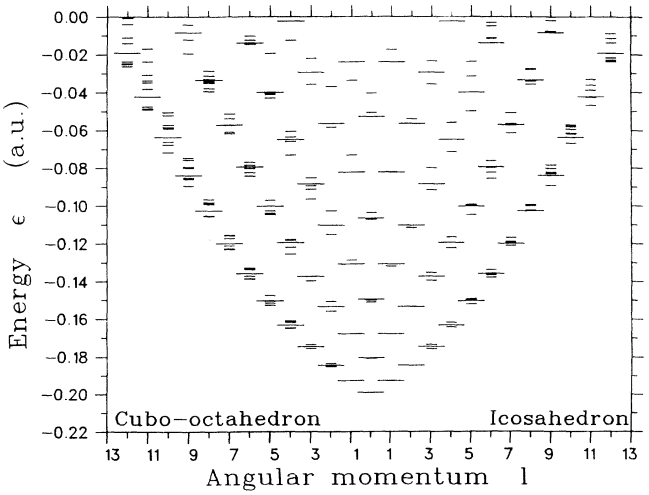

FIG. 1. Level structure of a 309-atom sodium cluster approximated with a square-well potential. For the nonspherical clusters the angular momentum is only approximately correct. The long lines represent the levels of the spherical well, the short lines on the left-hand side represent the levels of the cuboctahedral well, and those on the right-hand side represent the levels of the icosahedral well.

cuboctahedral potential wells corresponding to clusters with 309 atoms. The levels are shown as a function of the angular momentum eigenvalue. In the polyhedral wells, the angular momentum is not a good quantum number and the angular momentum shown corresponds to that of the maximum amplitude in the expansion with the spherical solutions. The degeneracy of each level, $2l+1$ (plus the spin degeneracy) in the spherical case, will be removed since the maximum degeneracy in the cubic cuboctahedral symmetry group is three and in the icosahedral one it is five. The splitting of the energy levels increase with increasing angular momentum and radial quantum number. In the case of the icosahedral cluster the splitting remains smaller than the energy difference between the different shells, whereas for the cuboctahedron the splitting is about the same magnitude as the difference between the shells. Figure 1 demonstrates that the icosahedral 309-atom cluster will have the main shell structure closely similar to that of the spherical cluster. However, it would be interesting to compare the predicted subshell behavior in detail to the experimental mass spectra.

We compare in Fig. 2 Fermi energies of complete icosahedral, cuboctahedral, and spherical clusters of different sizes. The Fermi energy changes between -0.083 a.u. $\leq \epsilon_F \leq -0.070$ a.u., when the cluster sizes change between $147 \leq N \leq 1415$. The Fermi energy depends more on the electronic shell in which it is located than on the cluster size. In our model the Fermi energy is the inverse of the ionization potential. The nonmonotonous behavior is an indication of the electronic-shell effects. Experimentally,[10] the icosahedral structures have been observed for clusters with a minimum in the ionization potential as a function of the cluster size. We have not addressed this topic, since a proper evaluation of the ionization potential of a rough surface requires a self-consistent calculation of the surface dipole layer.[20] For the spherical jellium clusters with about 1000 atoms we have estimated that the variation of the ionization potential due to the electronic-shell structure is about 0.2 eV. This is slightly more than the variation due to the geometry for the 1415-atom cluster seen in Fig. 2.

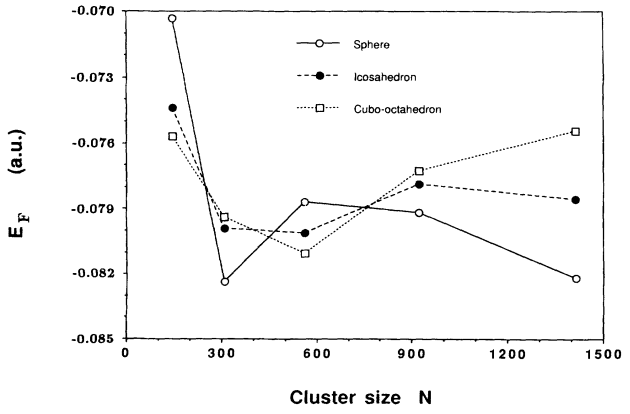

FIG. 2. Calculated Fermi energy for clusters with various sizes and geometries.

In large clusters, the main energy shells consist of a combination of several angular momentum values. It is then quite difficult to see the overall shell structure from the detailed scheme in Fig. 1. It is more illustrative to plot the density of states.[13] To this end we have smoothed the discrete levels with a Lorentzian

$$\rho(\epsilon)=\sum_{\nu}\frac{\Gamma}{(\epsilon-\epsilon_\nu)^2+\Gamma^2}\ , \tag{12}$$

where ϵ_ν is an individual eigenvalue. We have chosen the width $\Gamma=0.001$ a.u. Figures 3–6 show the densities of states for icosahedral and cuboctahedral sodium clusters with varying size. In each figure, the density of states of a spherical cluster with the same size is shown with a dashed line. The Fermi level (determined by the number of atoms in the cluster) changes from about -0.08 to -0.07 a.u. when the cluster size increases from 309 to 1415 atoms. We can see from Fig. 3 that the magic numbers are the same for the icosahedron and for the sphere

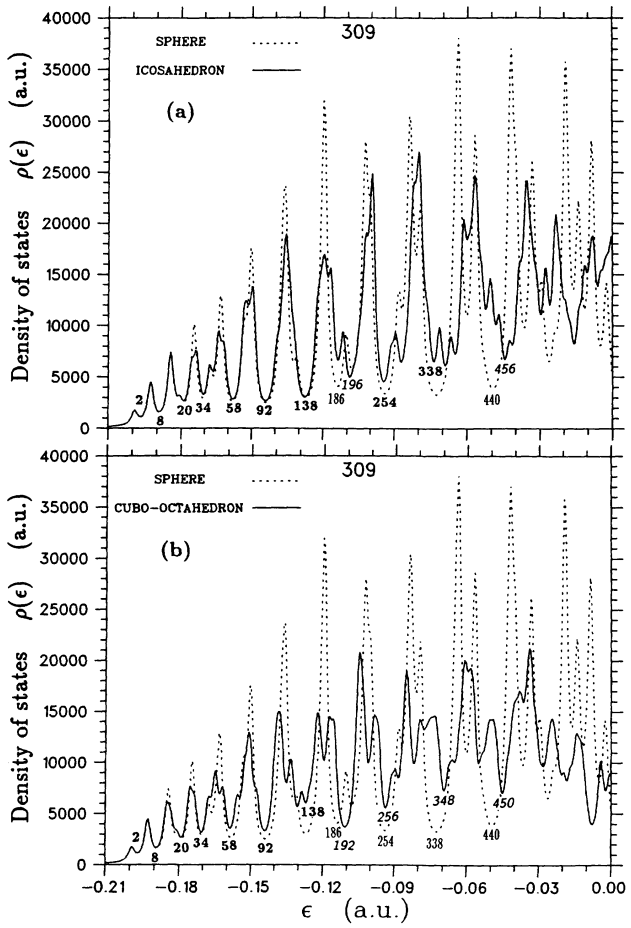

FIG. 3. Density of states of a 309-atom sodium cluster calculated for a spherical (dashed lines), (a) icosahedral, (b) cuboctahedral square well. The discrete levels have been convoluted with a Lorentzian. The numbers below the energy gaps indicate the corresponding magic numbers. Italic numbers denote the magic numbers for the icosahedral or cuboctahedral potential. A boldface number is used when the spherical and polyhedral potential give the same magic number.

still above the Fermi level. However, we notice that in details the subshell behavior in the two cases is different. For the cuboctahedron, only the lowest energy levels are the same as in the sphere. The level structure of the smallest cuboctahedral clusters agree with that obtained by Martins[21] using an *ab initio* pseudopotential approach.

For clusters from 561 to 1415 atoms, we have calculated only the shell structure close to the Fermi level. From Figs. 4 and 5 we can see that up to the Fermi energy the main shell structure of the icosahedral clusters is still quite similar to that of a sphere. The exact numbers corresponding to the shell fillings are somewhat different, however. It should be noted that the grouping of the levels of different angular momentum values is sensitive to the exact profile of the spherical potential: For example, a Wood-Saxon potential gives slightly different magic numbers than the square-well potential. It is not surprising, then, that when the spherical potential is replaced with an icosahedral potential, the exact magic numbers can change even if the shell structure is still very similar to that of a sphere. This is clearly seen in the case of the 309-atom cluster, where the sphere gives a deeper minimum for the shell closing at 186 electrons, whereas in the case of the icosahedral cluster the competing minimum at 196 electrons is deeper.

In the case of the 923-atom cluster, the shell structure of the sphere is not as clear as for the bigger 1415-atom cluster (Fig. 6). This is a supershell effect. The node between the first and second supershells in the square-well potential corresponds to a cluster with about 1000 atoms. In the 1415-atom icosahedral cluster, the shell structure is already markedly different from that of the spherical cluster.

In the case of the cuboctahedral clusters, the results are only approximative for clusters with more than 561 atoms due to the approximation made in Eq. (5). However, Figs. 2–4 clearly demonstrate that the disturbance to the shell structure is much larger than in the case of the icosahedral clusters.

The existence of the electronic-shell structure is a necessity for observing its effects, for example, on the mass spectra. However, total-energy calculations are needed for answering the question of whether the electronic-shell structure or the cluster geometry (atomic-shell structure) determines the most stable clusters. Many authors have tried to solve this problem with models based on the spherical jellium approximation.[18,22–25] However, as shown earlier[23,24] these models have the drawback that they exclude the possibility of crystalline ground-state structure, since the surface is forced to be spherical. Moreover, if these models are used for the crystalline geometry the surface energy of

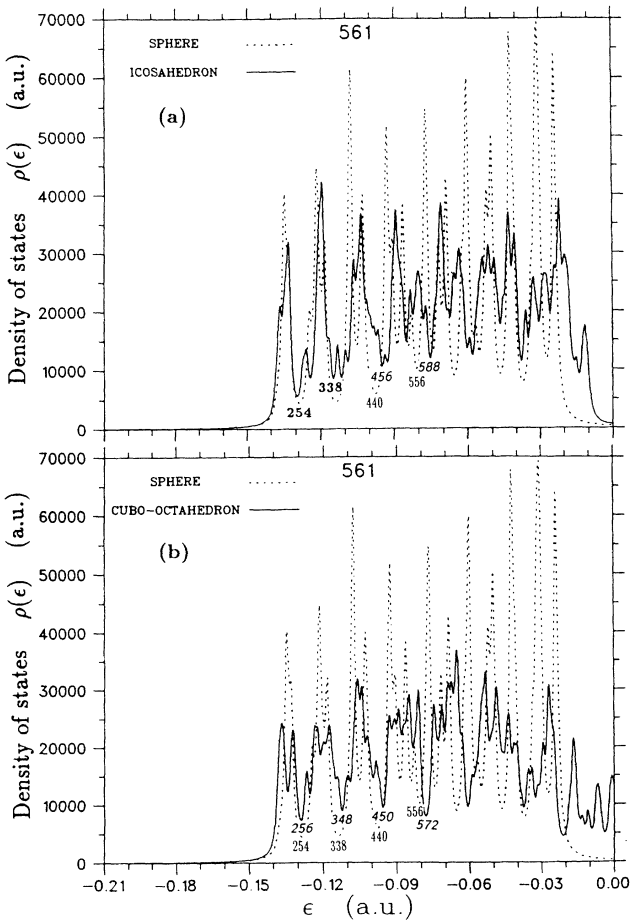

FIG. 4. Density of states for 561-atom sodium clusters.

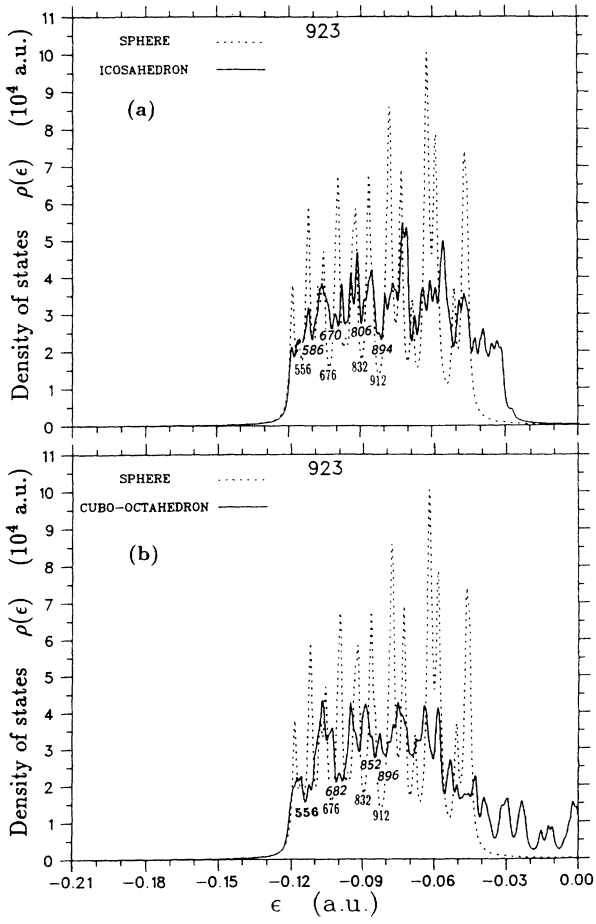

FIG. 5. Density of states for 923-atom sodium clusters.

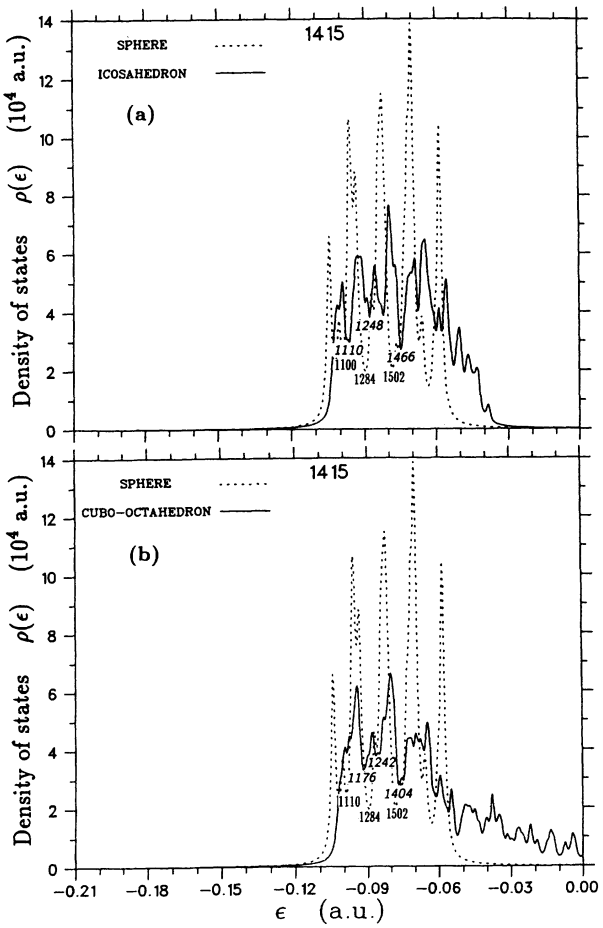

FIG. 6. Density of states for 1415-atom sodium clusters.

the cluster is strongly overestimated in large spherical clusters. In fact, the same problem arises in calculating the formation energy of spherical voids in bulk metals.[26] Thus, we believe that the recent prediction of Maiti and Falicov,[18] concerning the transition from electronic- to geometry-determined magic numbers when the cluster size exceeds 100 atoms, is not conclusive.

IV. LIQUID CLUSTERS: QUADRUPOLE DEFORMATION

The large magic numbers corresponding to the electronic-shell structure have been observed for warm clusters[7] that could be in liquid state. The surface tension will force the liquid clusters to be spherical but at finite temperatures there will be fluctuations at the surface structure. Using the potential-well approximation, we can study the effects of such surface waves on the electronic-shell structure. The energy of the surface-wave excitation can be estimated from the change in the surface energy. In a more accurate description, the change of curvature energy could also be included.[27]

In a small cluster, there is an interplay between the shell structure and the deformation (Jahn-Teller effect) of the clusters that has been studied using spheroidal (quadrupole),[28,29] or recently also with octupole, deformations.[30] Since we are concentrating on large clusters, the shell-structure effects on the deformation can be neglected. For simplicity, we assume the liquid to be incompressible. The equipartition theorem requires that each surface model has an energy of the order

$$E_{\rm sw}=k_B T \ . \tag{13}$$

The energy of the surface wave can be estimated from the increase of the surface area ΔA:

$$E_{\rm sw}=\sigma \Delta A \ , \tag{14}$$

where σ is the surface tension (for sodium, $\sigma=200$ erg/cm^2). The long-wavelength limit of the surface wave corresponds to the quadrupole deformation, where the sphere deforms to a spheroid. The change in the surface area ΔA and the volume for a prolate spheroid with semiaxes a and b and eccentricity ϵ can be written as

$$\Delta A = A_{\rm spd} - A_{\rm sph} = 2\pi b^2 + 2\pi \frac{ab}{\epsilon} \arcsin\epsilon - 4\pi r_0^2 N^{2/3} \ , \tag{15}$$

$$V=\tfrac{4}{3}\pi a b^2 \ .$$

Defining the "amplitude" of the surface wave by $x=(b-r_0)/r_0$, it is straightforward to derive from Eqs. (14) and (15) that for small deformations

$$E_{\rm sw} \propto r_0^2 x^2 \ . \tag{16}$$

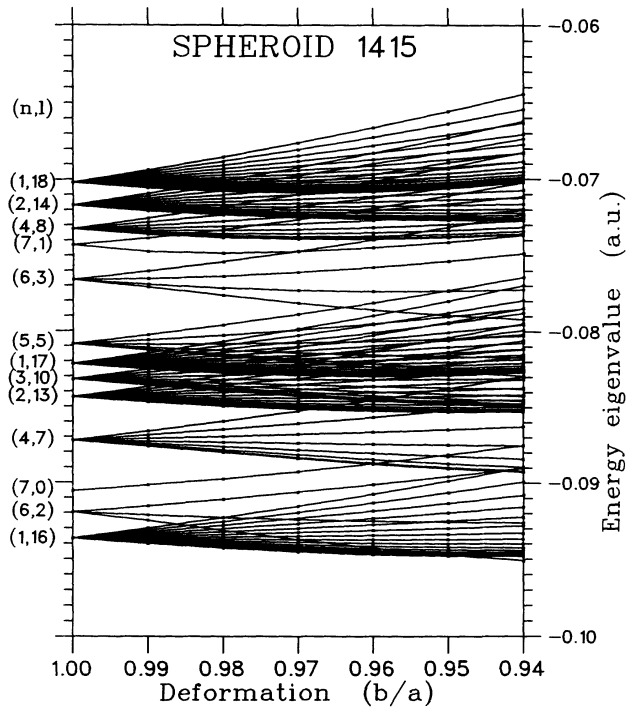

FIG. 7. Single-electron energy levels for a prolate spheroidal potential well as a function of the deformation (b/a). The numbers in parentheses show the radial and angular quantum numbers (n,l) of the level in a spherical potential ($n=1$ corresponds to the lowest state for each angular momentum).

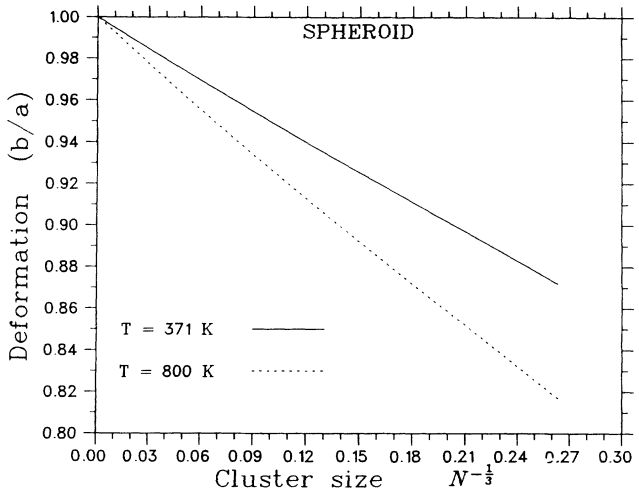

FIG. 8. The average instantaneous quadrupole deformation of a liquid sodium cluster as a function of the cluster size. The calculation is based on the assumption that the deformation energy equals $k_B T$.

From Eqs. (7) and (8) we notice that the change in the energy eigenvalues due to the deformation

$$\Delta\epsilon \propto \frac{x}{r_0} . \tag{17}$$

Combining Eqs. (13), (16), and (17), and using the fact that $r_0 \propto N^{1/3}$, we get the following important result:

$$\Delta\epsilon \propto \frac{\sqrt{k_B T}}{N^{2/3}} . \tag{18}$$

This means that for a given temperature the effect of the surface waves on the energy levels *decreases* when the cluster size increases. The energy difference between the major shells in a spherical cluster is proportional to $N^{-1/3}$. The relative disturbance of the surface waves on the shell structure decreases when the cluster size increases and depends only weakly on the temperature.

Figure 7 shows the level structure of a 1415-atom cluster as a function of the degree of the deformation (b/a ratio). Only the prolate case and the levels close to the Fermi level were considered. Figure 8 shows the average deformation determined by Eqs. (13)–(15) for two

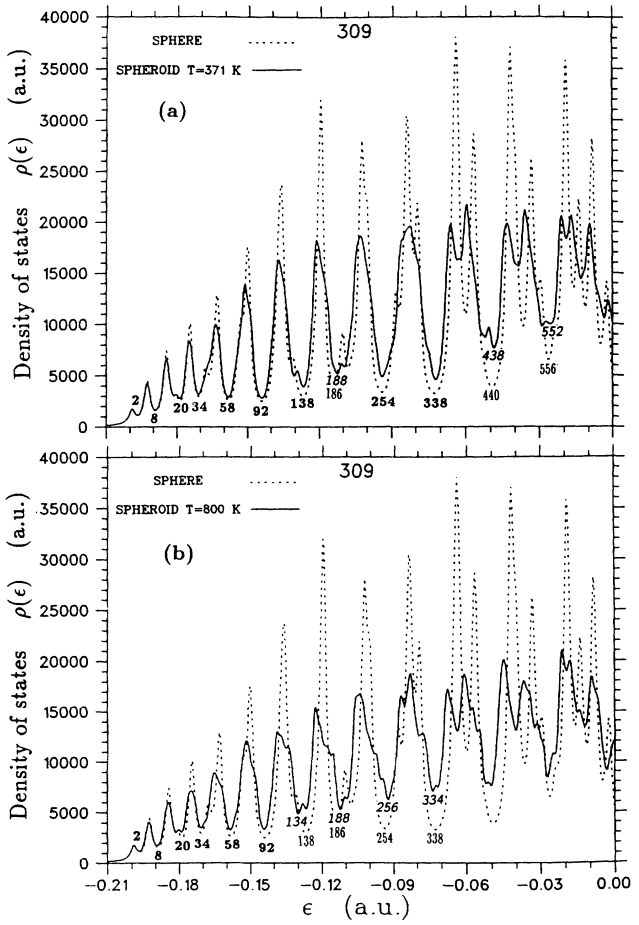

FIG. 9. Density of states of a spheroidal 309-atom sodium cluster. The two deformations correspond to temperatures of (a) 371 K and (b) 800 K.

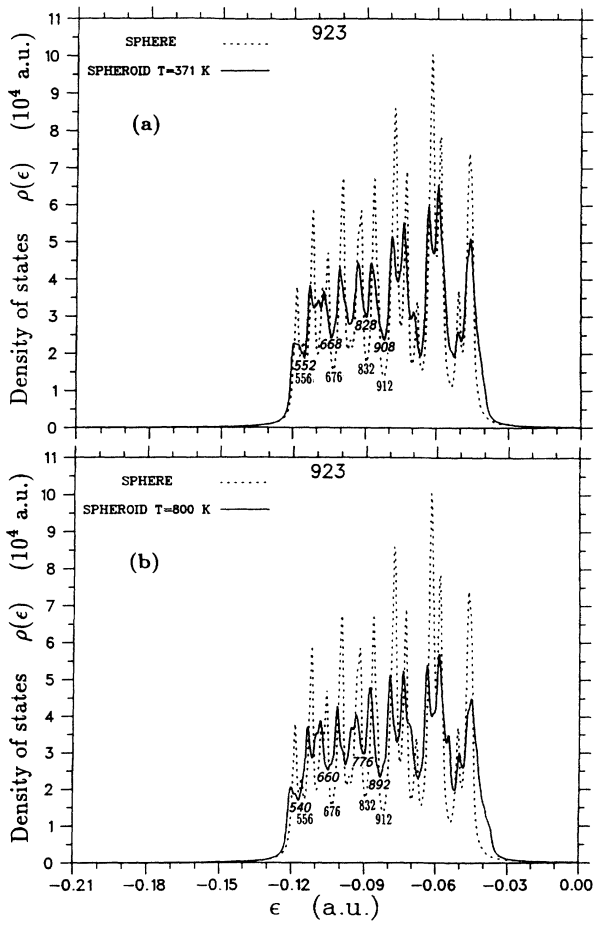

FIG. 10. Density of states of a spheroidal 923-atom sodium cluster. The two deformations correspond to temperatures of (a) 371 K and (b) 800 K.

different temperatures, 800 and 371 K (the melting point of bulk sodium). At the melting temperature the deformation for the 1415-atom cluster is about 0.955 and, consequently, the main shell structure still clearly prevails. Due to the grouping of the levels, the main features of the shell structure remain prominent even at $b/a=0.935$, which corresponds to the temperature of about 800 K.

Figures 9 and 10 show the density of states for prolate spheroids corresponding to 309- and 923-atom sodium clusters. In each case, densities for two deformations are shown, one corresponding to an average instantaneous deformation in 800 K and one for the melting temperature. In both clusters the effect of the deformation is fairly small even at the higher temperature. A comparison with Figs. 3 and 5 shows that the liquid clusters are expected to be much more spherical than the solid icosahedral or cuboctahedral clusters.

We have only considered the simplest surface-wave mode, the spheroidal deformation. In a real sample of clusters, many different surface modes will exist. However, the energy of any higher multipole mode estimated from the surface energy corresponds to an amplitude smaller than that of the quadrupole mode. This follows from the faster increase of the surface area for the higher multipoles. It is then expected that the quadrupole mode has the largest effect on the shell structure of liquid clusters. The higher temperature considered 800 K is already difficult to achieve in small clusters, since they would start to evaporate atoms. We can then conclude that the surface fluctuations in liquid sodium clusters do not destroy the main features of the electronic-shell structure.

V. CONCLUSIONS

We have used a simple square-well-potential model to study the effects of the cluster shape on the electronic-shell structure. In the cuboctahedral clusters, the shell structure already differs markedly from that of the sphere when the cluster has less than 300 atoms. The icosahedral shape sustains the basic features of the spherical-shell structure up to about 1000 atoms in the cluster. These conclusions are in agreement with the earlier Hückel model calculations.[13]

The effect of the quadrupole deformation has been studied in some large clusters. By estimating an average deformation of a surface wave from the surface tension and from the equipartition theorem, we have shown that the surface fluctuations in liquid clusters do not destroy the main electronic-shell structure. The relative effect of the surface fluctuations on the shell structure becomes smaller when the cluster size increases.

ACKNOWLEDGMENTS

We would like to thank S. Bjørnholm, B. Mottelson, J. Suhonen, and T. P. Martin for many valuable discussions. This work was supported by the Academy of Finland.

[1]J. Martins and J. Buttet, Surf. Sci. **106**, 261 (1981).
[2]A. Hintermann and M. Manninen, Phys. Rev. B **27**, 7262 (1983).
[3]W. Ekard, Phys. Rev. B **29**, 1558 (1984).
[4]W. A. de Heer, W. D. Knight, M. Y. Chou, and M. L. Cohen, Solid State Phys. **40**, 93 (1987).
[5]S. Bjørnholm, Contemp. Phys. **31**, 309 (1990).
[6]W. D. Knight, K. Clemenger, W. A. de Heer, W. A. Saunders, M. Y. Chou, and M. Cohen, Phys. Rev. Lett. **52**, 2141 (1984).
[7]J. Pedersen, B. Bjørnholm, J. Borggren, K. Hansen, T. P. Martin, and H. D. Rasmussen, Nature **353**, 733 (1991).
[8]*Theory of Inhomogeneous Electron Gas,* edited by S. Lundqvist and N. H. March (Plenum, New York, 1983).
[9]H. Nishioka, K. Hansen, and B. R. Mottelson, Phys. Rev. B **42**, 9377 (1990).
[10]T. P. Martin, T. Bergmann, H. Göhlich, and T. Lange, Chem. Phys. Lett. **172**, 209 (1990).
[11]T. P. Martin, T. Bergmann, H. Göhlich, and T. Lange, Chem. Phys. Lett. **176**, 343 (1991).
[12]T. P. Martin, U. Näher, T. Bergmann, H. Göhlich, and T. Lange, Chem. Phys. Lett. **183**, 119 (1991).
[13]J. Mansikka-aho, M. Manninen, and E. Hammarén, Z. Phys. D **21**, 271 (1991).
[14]V. Bonaĉiĉ-Koutecký, P. Fantucci, and J. Koutecký, Chem. Rev. **91**, 91 (1991).
[15]U. Röthlisberger and W. Andreoni, J. Chem. Phys. **94**, 8129 (1991).
[16]O. B. Chistensen, K. W. Jacobsen, J. K. Nørskov, and M. Manninen, Phys. Rev. Lett. **66**, 2219 (1991).
[17]M. P. Iñigues, M. J. López, J. A. Alonso, and J. M. Soler, Z. Phys. D **11**, 163 (1989).
[18]A. Maiti and L. M. Falicov, Phys. Rev. A **44**, 4442 (1991).
[19]M. Manninen and P. Jena, Europhys. Lett. **14**, 643 (1991).
[20]R. Monnier and J. P. Perdew, Phys. Rev. B **17**, 2595 (1978).
[21]J. L. Martins, Z. Phys. D **12**, 347 (1989).
[22]J. Martins and J. Buttet, Surf. Sci. **106**, 261 (1981).
[23]M. Manninen, Solid State Commun. **59**, 281 (1986).
[24]M. Manninen, in *Condensed Matter Theories,* edited by J. Arponen, R. F. Pishop, and M. Manninen (Plenum, New York, 1988), Vol. 3.
[25]A. Mañanes, J. A. Alonso, U. Lammers, and G. Borstel, Phys. Rev. B **44**, 7273 (1991).
[26]M. Manninen and R. M. Nieminen, J. Phys. F **8**, 2243 (1978).
[27]J. P. Perdew, Y. Wang, and E. Engel, Phys. Rev. Lett. **66**, 508 (1991).
[28]K. Clemenger, Phys. Rev. B **32**, 1359 (1985).
[29]Z. Penzar and W. Ekardt, Z. Phys. D **17**, 69 (1990).
[30]I. Hamamoto, B. Mottelson, H. Xie, and X. Z. Zhang, Z. Phys. D **21**, 163 (1991).